LETTER • OPEN ACCESS

High-thermal-stability resistor formed from manganese nitride compound that exhibits the saturation state of the mean free path

To cite this article: Hisashi Kino *et al* 2021 *Appl. Phys. Express* **14** 091003

Applied Physics Express **14**, 091003 (2021) LETTER
https://doi.org/10.35848/1882-0786/ac18b0

High-thermal-stability resistor formed from manganese nitride compound that exhibits the saturation state of the mean free path

Hisashi Kino[1*], Takafumi Fukushima[2,3], and Tetsu Tanaka[2,3]

[1]Frontier Research Institute for Interdisciplinary Sciences, Tohoku University, Sendai, Miyagi 980-8579, Japan
[2]Depertment of Mechanical Systems Engineering, Tohoku University, Sendai, Miyagi 980-8579, Japan
[3]Graduate School of Biomedical Engineering, Tohoku University, Sendai, Miyagi 980-8579, Japan

[*]E-mail: kino@lbc.mech.tohoku.ac.jp

Received June 28, 2021; revised July 22, 2021; accepted July 27, 2021; published online August 10, 2021

Antiperovskite manganese nitride compounds possess the saturation characteristics of the mean free path at an approximate room temperature. Therefore, such compounds show a flat resistance–temperature curve at an approximate room temperature. In this paper, we propose a manganese nitride resistor for high-thermal-stability systems. We fabricated and evaluated the micro/nanoscale manganese nitride compound resistors using the complementary metal-oxide-semiconductor-compatible process. The thermal coefficient of the fabricated manganese nitride compound resistor was as low as that of other near-zero temperature-coefficient of resistivity materials. These results indicate that manganese nitride compounds can achieve higher thermal stability.

Complementary metal-oxide-semiconductor (CMOS) integrated circuits (ICs) have been widely used in various devices and equipment, such as mobile phones, automobiles, and medical devices. This fact indicates that CMOS ICs can be used under varying temperatures. The heat generation due to circuit operations also results in IC performances with critical issues.[1–4] The thermal stability of CMOS ICs is one of the important characteristics that ensures their use at different ambient temperatures. The resistances of conductive materials (e.g. Al, Cu, TiN) increase when heated owing to the increase in carrier scattering. By contrast, the resistances of semiconductor materials decrease when heated owing to carrier generation. These changes in resistance lead to an increase in power consumption and the area for the redundancy circuits.[5,6] Most fields of application require CMOS ICs with high thermal stability. In this study, to achieve high thermal stability, we focused on the saturation phenomena of the mean free path, which is decreased by an increase in the carrier scattering. The results of the proposed technique can provide passive components with high thermal stability, such as poly-Si resistors used in electrostatic discharge protection circuits and voltage reference circuits.[7,8)]

Electrical resistivity varies inversely with the mean free path of an electron. In general, the mean free path is reduced by an increase in temperature. The mean free path is usually much larger than the separation of the atoms, and most materials exhibit the saturation characteristics of the mean free path close to their melting points or at higher temperatures. However, a considerably limited number of materials exhibit constant electrical resistivity with changes in temperature, and a near-zero temperature-coefficient of resistivity (NZ-TCR) behavior at an approximate room temperature.[9–13] In such materials, the mean free path reaches the separation of the atoms.[14,15]

An antiperovskite manganese nitride is one of the materials which show NZ-TCR at an approximate room temperature.[16,17] Antiperovskite manganese nitride compounds have several unique characteristics, which other NZ-TCR materials do not possess, such as exceptionally high negative thermal expansion and magnetocaloric effects.[18–23] The effects of thermal stress induced by the multilevel interconnects on the reliability of ICs increase every year. This thermal stress, which causes wafer bowing and stress migration of the wirings, is induced by the mismatch in coefficient of thermal expansion (CTE) between the multilevel interconnects and the Si substrate. By compounding a positive CTE material with a negative one, the total CTE can approach zero. Thus, we can expect that manganese nitride compound materials with a negative CTE can suppress the thermal stress induced by the back end of line (BEOL) process. For instance, attempts have been made to exploit this exceptionally high negative thermal expansion characteristic of manganese nitride compounds in the IC packaging field.[24–26] Because of these unique advantages, we focused on the manganese nitride compounds having low TCR at an approximate room temperature. Figure 1 shows the antiperovskite crystal structure where the atom shown as X is Cu, Zn, Ge. It is considered that the mean free path is comparable to the interatomic separations in the antiperovskite manganese nitride.

In this study, we attempted to apply the manganese nitride material to the resistors used for resistance adjustment in CMOS ICs to achieve a high thermal stability system. For use in CMOS ICs, we fabricated the micro/nanoscale-width manganese nitride resistors by using a CMOS-compatible process, which includes conventional sputtering, patterning, annealing, and wet processes. We reported on the fundamental characteristics of the micro/nanoscale-width manganese nitride resistors fabricated through the CMOS-compatible process.

We fabricated the micro/nanoscale manganese nitride compound resistors by using a CMOS-compatible process that includes a typical sputtering system; the process flow is shown in Fig. 2. Firstly, we performed the thermal oxidation process. We then formed the resistor pattern using an electron-beam (EB) resist. Thereafter, we fabricated the resistors with the lift-off process using the EB resist and a polymethylglutarimide (PMGI) sacrificial layer. This combination is usually used for the T-shaped gate electrodes of the high electron mobility transistors.[27–29] Subsequently, the manganese nitride compound layer was deposited by a depo-up type radio frequency magnetron sputtering system. We used the manganese nitride compound target, which includes

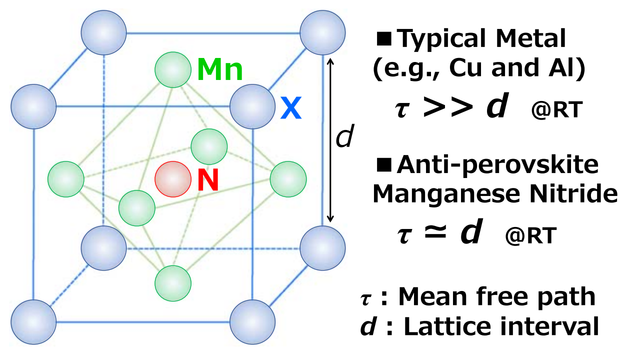

Fig. 1. (Color online) Crystal structure of manganese nitride compounds with antiperovskite structure.

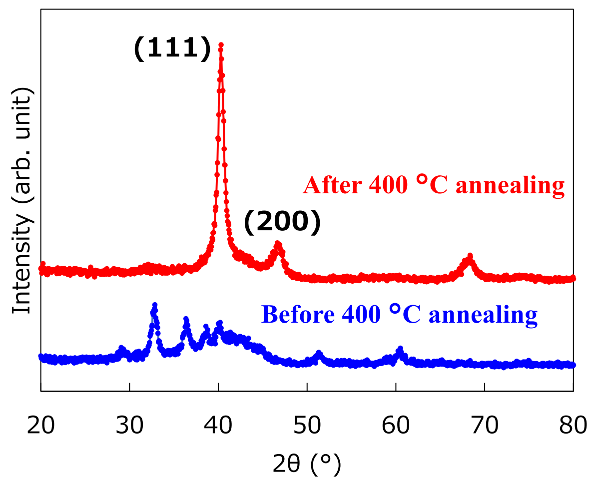

Fig. 3. (Color online) XRD measurement results of the manganese nitride compound thin film deposited by the typical sputtering system before and after 400-°C annealing.

tin and zinc, as the atom X shown in Fig. 1. The compositional ratio between tin and zinc was 1:2. This ratio can affect the temperature range which shows low TCR. We used the ratio that shows low TCR at and around room temperature. The sputtering pressure, power, and temperature were 0.5 Pa, 50 W, and room temperature, respectively. Argon gas, having a flow rate of 20 sccm, was used for sputtering. We obtained a deposition rate of 13.5 nm min^{-1} in this condition. We then fabricated the manganese nitride compound resistors with the lift-off process by removing the EB resist and PMGI. Finally, the samples were annealed at 400 °C in an argon atmosphere of 5 Pa to obtain the antiperovskite crystalline. A temperature of 400 °C is widely used for the annealing process, such as H_2 sintering, which is the process having the highest temperature in the BEOL. Therefore, this crystallization annealing process does not affect the other elements and processes in the BEOL. Then, other processes in BEOL do not also affect the manganese nitride resistors. We annealed the sample under a low-pressure environment to avoid chemical reactions. The right-bottom image in Fig. 2 shows the scanning electron microscope (SEM) image of the fabricated resistor. We then validated the micro/nanoscale resistor produced from the manganese nitride compound.

Figure 3 shows the X-ray diffraction (XRD) spectrum of the manganese nitride compound thin film before and after the 400 °C-annealing. The thickness of the sputtered manganese nitride thin film was 200 nm. The XRD spectrum of the sample before the annealing process did not show the antiperovskite manganese nitride compounds. The spectrum was remarkably similar to the structure of $ZnMn_2O_4$. The base pressure of the sputtering process was approximately 4×10^{-6} Pa. There is a possibility that the base pressure was not quite low. However, the value is typical for the conventional sputtering system. Therefore, to fabricate the manganese nitride compound resistor by using a CMOS compatible process, it is preferable to form antiperovskite manganese nitride compounds by using typical base pressure. The peak position and intensity ratio of the sample after the annealing process were similar to those of the antiperovskite manganese nitride compounds produced via the sintering method.[9,19,30,31] This result indicates that the 400 °C annealing process can produce a sputtered manganese nitride thin film with an antiperovskite structure. It also shows that we can fabricate the micro/nanoscale manganese nitride resistor having an antiperovskite structure using a CMOS-compatible process.

Firstly, for the purpose of comparison, we measured the resistance of the aluminum wirings, which were fabricated using the same process. The design value of the width of the

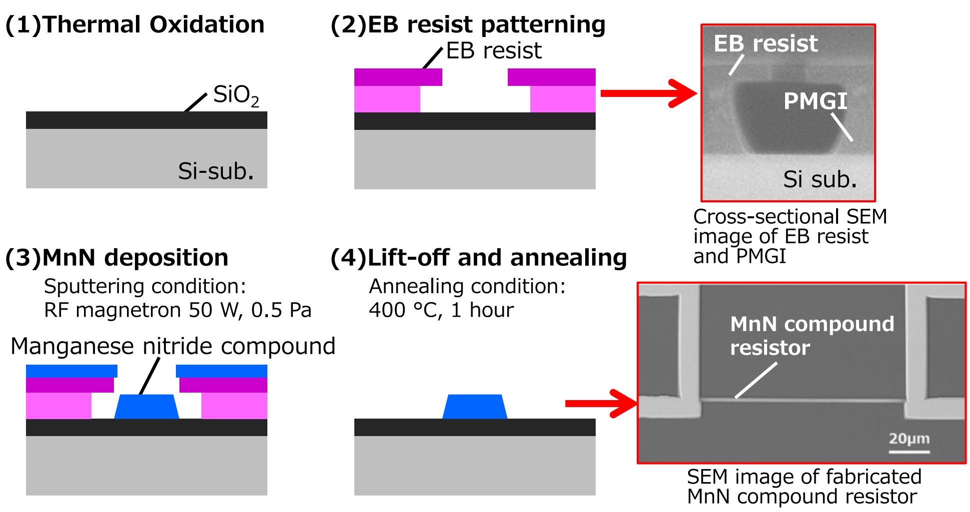

Fig. 2. (Color online) Process flow of the manganese nitride compound resistors and SEM image of the fabricated manganese nitride compound resistor.

wiring was 0.8 μm. We then measured the resistance of the poly-Si resistors, which were fabricated using a plasma etching process. The dopant was phosphorus, and the concentration was 1×10^{20} cm^{-3}. The results of measuring the voltage–current characteristics at different temperatures are shown in Fig. 4. We evaluated the resistance of each material using the bridge test structure, which can perform four-terminal measurement and avoid parasitic resistance. The B1500A semiconductor parameter analyzer was used as the measurement instrument. The measurements were performed at a temperature range of 30 °C–50 °C, and at 5 °C intervals. We observed an increase in resistance in the aluminum wirings and a decrease in the poly-Si resistors. Such resistance changes were induced by an increase in carrier scattering and carrier generation caused by an increase in temperature.

Figure 4(c) shows the results of measuring the voltage–current characteristics of the fabricated manganese nitride compound resistor. The design value of the width of the resistor was also 0.8 μm. The thickness was 80 nm. The measurements were carried out at a temperature range of 30 °C−100 °C, at 10 °C intervals. Considerably limited changes in the resistance were observed due to the change in temperature even though the measurement temperature was wider than that of the aluminum wiring and poly-Si resister. The resistivity of the manganese nitride compound resistor was approximately 300 $\mu\Omega$ cm, which was almost the same as the resistivity of the antiperovskite manganese nitride compounds produced via the sintering method.[9,16] The resistivity was also similar in the order of the highly doped poly-Si resistor. This means that we can design the layout of the manganese nitride resistor like we design a conventional poly-Si resistor.

Figure 5 (left) shows the effect of the temperature change on the resistance change ratio. The TCRs of the aluminum wiring and poly-Si resistor were 1162 ppm °C^{-1} and −1188 ppm °C^{-1}, respectively. Herein, the TCRs were calculated using the regression line of the results shown in Fig. 5 (left). The minor reduction in the resistance of the manganese nitride compound resistors was considered to be induced by the carrier generation close to the Fermi level.[22] However, the manganese nitride compound is not a semiconductor with an energy gap.[16] Therefore, we believe that the effect of carrier generation was minimal. The TCR of the manganese nitride compound resistor with an 800 nm width and an 80 nm thickness was approximately −54 ppm °C^{-1}, which was 1/20 times less than that of the aluminum wirings and poly-Si resistors. The resistance change ratio from 30 °C to 100 °C was used for calculating the TCR of the manganese nitride compound resistors.

We performed the accelerated aging test with a current density of 1 MA cm^{-2} under a temperature of 80 °C in the atmospheric air. Considerably limited changes in the resistance were observed due to the thermal and current stress. This result indicates that the manganese nitride compound resistor has a high migration resistance. However, a minor increase in the resistance was also noticed. It is likely that these behaviors, as shown in Fig. 5, were induced by the chemical reactions between the atmospheric air and the surface of the manganese nitride compound resistor, which include hydrolysis and oxidation. In the case of actual ICs, the resistors are passivated by the interlayer dielectric, such as SiO_2 or SiN. Therefore, we can consider that the reactions between the manganese nitride resistors and atmospheric air are suppressed in actual ICs. These results indicated that the manganese nitride compound deposited by a typical sputtering system could also display low TCR behavior at an approximate room temperature and high migration resistance.

Table I shows the comparison between materials having low TCR; the TCR of the fabricated manganese nitride compound resistor is not the lowest among these materials. In contrast, some deposition methods, such as atomic layer deposition (ALD), lead to higher process cost. Thinner film thickness also leads to a large variation in the resistance of the resistors. Therefore, we can consider that manganese nitride compounds show suitable characteristics for BEOL

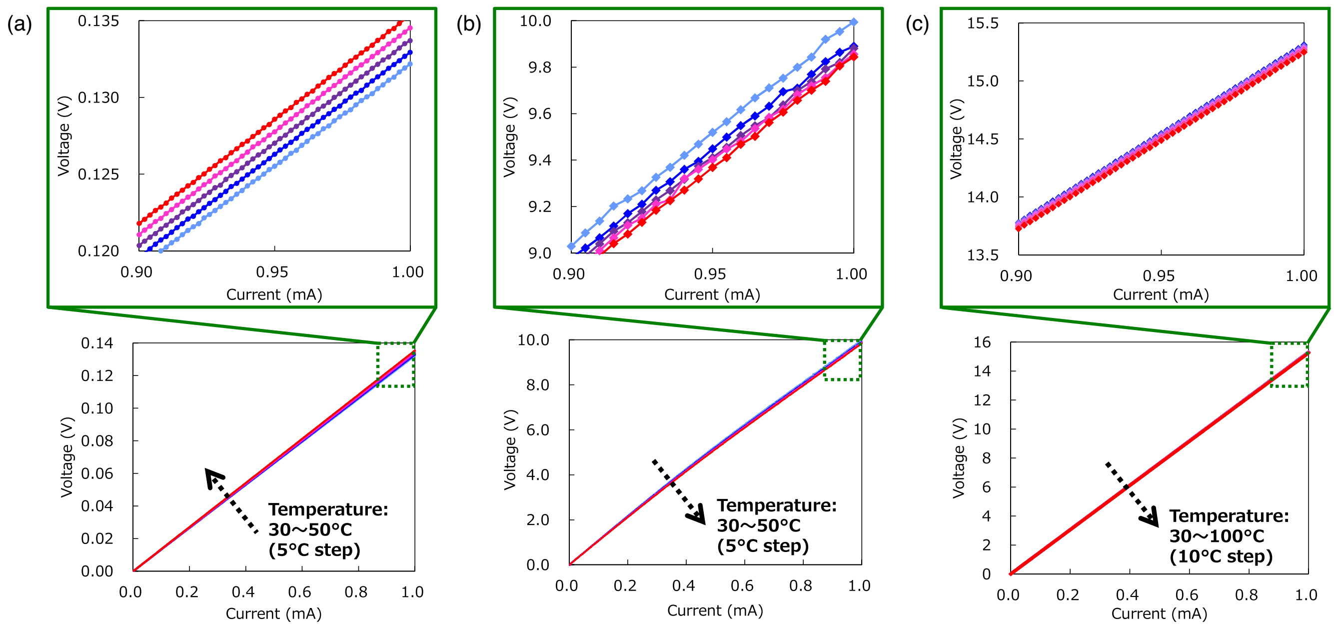

Fig. 4. (Color online) Voltage–current characteristics of (a) the Al wiring, (b) poly-Si resistor, and (c) manganese nitride compound resistor under the temperature changes.

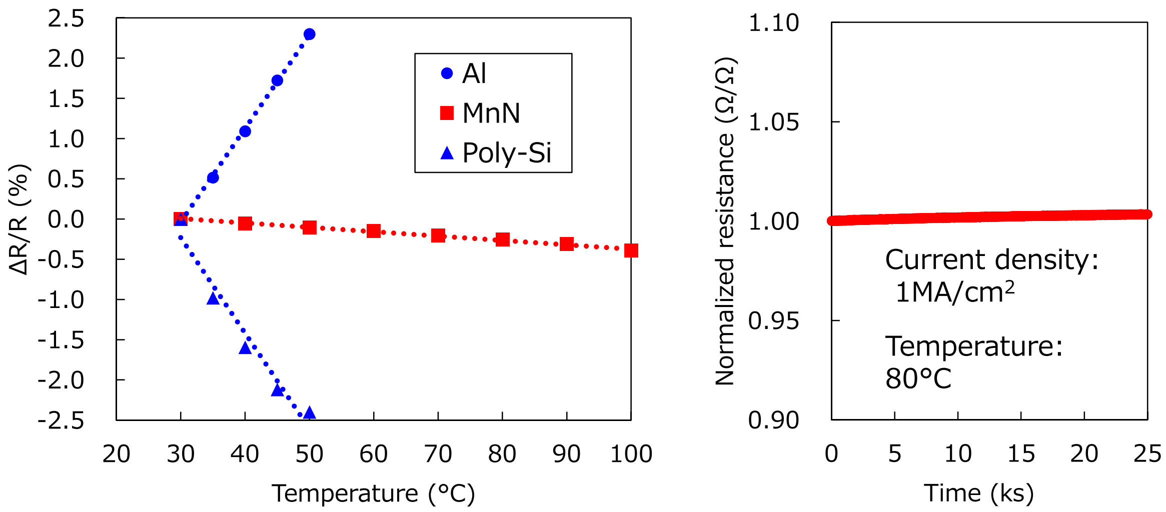

Fig. 5. (Color online) Temperature dependence of the resistance-change ratio of the fabricated manganese nitride compound resistor, the Al wiring, and poly-Si resistor (left), and the result of the accelerated aging test of manganese nitride compound resister (right).

Table I. Comparison between low-TCR materials.

Material	MnN	$TiSi_xN$	SiCr	Ta_2N	TiAlN	NiCr	MnN
TCR (ppm K^{-1})	3.1	−23	−3.9	−103	−765.4	<10	−54
Deposition method	Sintering	ALD	Sputtering	Reactive sputtering	co-sputtering	Sputtering	Sputtering
Process temp. (°C)	800	450	400	—	400	375	400
Thickness (nm)	Bulk (Powder)	139.6	3–4	44	200	10	80
References	17	15	10	11	12	13	This work

with respect to the deposition method, process temperature, and thickness that can indicate low TCR. In addition, manganese nitride compounds exhibit negative CTEs, which makes it possible to suppress the thermal stress induced by the mismatch in CTE between the multilevel interconnects and the Si substrate. Therefore, these results indicate that manganese nitride compounds are one of the promising materials for application as resistors to realize high-thermal-stability ICs.

We demonstrated that manganese nitride compound resistors, fabricated using a CMOS-compatible process, exhibit low TCRs at approximate room temperatures. The measurement results indicated that the manganese nitride compounds have the ability to realize higher thermal-stability ICs compared to conventional aluminum wirings and poly-Si resistors. The fabricated manganese nitride compound resistors also show suitable characteristics for the BEOL process in ICs. Further studies, including the evaluation of negative CTE effects on the thermal stress in ICs, and reducing the TCR of manganese nitride compounds by considering the post-annealing process, deposition conditions, and nanoscale size effect are required.

Acknowledgments This work was supported by JSPS KAKENHI under grant number 20H02193 and the Frontier Research Institute for Interdisciplinary Sciences (FRIS) at Tohoku University, and through the activities of VDEC, The University of Tokyo, in collaboration with Cadence Design Systems. The work was performed in the Micro/Nano-Machining Research and Education Center at Tohoku University.

1) S. Pal and A. Islam, IEEE Trans. Device Mater. Reliab. **16**, 172 (2016).
2) H. Kino, H. Hashiguchi, S. Tanikawa, Y. Sugawara, S. Ikegaya, T. Fukushima, M. Koyanagi, and T. Tanaka, Jpn. J. Appl. Phys. **55**, 04EC03 (2016).
3) H. Kino, J.-C. Bea, M. Murugesan, K.-W. Lee, T. Fukushima, M. Koyanagi, and T. Tanaka, 2013 IEEE 63rd Electronic Components and Technology Conf. 2013, p. 360.
4) H. Kino, J. C. Bea, M. Murugesan, K. W. Lee, T. Fukushima, M. Koyanagi, and T. Tanaka, Jpn. J. Appl. Phys. **52**, 04CB11 (2013).
5) L. Peng, Y. Cao, X. Pan, and X. Zhao, 2017 Int. SoC Design Conf. 2017, p. 115.
6) J. Wang, W. L. Goh, X. Liu, and J. Zhou, IEEE Trans. Circuits Syst. I Regul. Pap. **63**, 1816 (2016).
7) C. Duvvury and R. Rountree, J. Electrostat. **29**, 1 (1992).
8) L. Cui, Proc. 2011 Int. Conf. on Electronic & Mechanical Engineering and Information Technology 2011, Vol. 4, p. 2187.
9) L. Ding, C. Wang, L. Chu, J. Yan, Y. Na, Q. Huang, and X. Chen, Appl. Phys. Lett. **99**, 251905 (2011).
10) Y.-C. Kwon, H.-C. Seol, S.-K. Hong, and O.-K. Kwon, IEEE Trans. Electron Devices **61**, 8 (2014).
11) T. Riekkinen, J. Molarius, T. Laurila, A. Nurmela, I. Suni, and J. Kivilahti, Microelectron. Eng. **64**, 289 (2002).
12) M.-H. Park and S.-H. Kim, Trans. Nonferrous Met. Soc. China **23**, 433 (2013).
13) D. Nachrodt, U. Paschen, A. ten Have, and H. Vogt, IEEE Electron Device Lett. **29**, 212 (2008).
14) O. Gunnarsson, M. Calandra, and J. E. Han, Rev. Mod. Phys. **75**, 1085 (2003).
15) C. Feit, S. Chugh, A. R. Dhamdhere, H. Y. Kim, S. Dabas, S. J. Rathi, N. Mukherjee, and P. Banerjee, J. Vac. Sci. Technol. A **38**, 062404 (2020).
16) T. Oe, C. Urano, N. Kaneko, M. Hadano, and K. Takenaka, Appl. Phys. Lett. **103**, 173518 (2013).
17) J. C. Lin, P. Tong, S. Lin, B. S. Wang, W. H. Song, and Y. P. Sun, J. Appl. Phys. **116**, 213912 (2014).
18) K. Takenaka and H. Takagi, Appl. Phys. Lett. **87**, 261902 (2005).
19) Z. Sun and X. Song, J. Mater. Sci. Technol. **30**, 903 (2014).
20) F. Yu, L. Ren, M. Meng, Y. Wang, M. Yang, S. Wu, and S. Li, J. Appl. Phys. **115**, 133911 (2014).
21) K. Takenaka, K. Asano, M. Misawa, and H. Takagi, Appl. Phys. Lett. **92**, 011927 (2008).
22) M. Kobayashi and M. Mochizuki, Phys. Rev. Mater. **3**, 024407 (2019).
23) M. Hadano, A. Ozawa, K. Takenaka, N. Kaneko, T. Oe, and C. Urano, J. Appl. Phys. **111**, 07E120 (2012).
24) H. Kino, T. Fukushima, and T. Tanaka, 2016 IEEE Int. 3D Systems Integration Conf. 2016, p. 1.

25) H. Kino, H. Hashiguchi, Y. Sugawara, S. Tanikawa, T. Fukushima, K. Lee, M. Koyanagi, and T. Tanaka, 2014 IEEE 64th Electronic Components and Technology Conf., 2014, p. 1110.
26) H. Kino, T. Fukushima, and T. Tanaka, 2019 Int. 3D Systems Integration Conf., 2019, p. 1.
27) Y. Chen, D. S. Macintyre, X. Cao, E. Boyd, D. Moran, H. McLelland, M. Holland, C. R. Stanley, I. Thayne, and S. Thoms, J. Vac. Sci. Technol. B **21**, 3012 (2003).
28) K.-S. Lee, K.-T. Lee, Y.-S. Kim, and Y.-H. Jeong, 5th IEEE Conf. on Nanotechnology, 2005, Vol. 2, p. 97.
29) B. Sun, P. Zhang, T. Zhang, S. Shangguan, S. Wu, and X. Ma, Microelectron. Eng. **229**, 111337 (2020).
30) K. Takenaka, M. Ichigo, T. Hamada, A. Ozawa, T. Shibayama, T. Inagaki, and K. Asano, Sci. Technol. Adv. Mater. **15**, 015009 (2014).
31) X. Guo, P. Tong, J. Lin, C. Yang, K. Zhang, S. Lin, W. Song, and Y. Sun, Front. Chem. **6**, 1 (2018).